Cluster Compounds

Deutsche Ausgabe: DOI: 10.1002/ange.201500590
Internationale Ausgabe: DOI: 10.1002/anie.201500590

Alkynyl-Protected Au_{23} Nanocluster: A 12-Electron System**

Xian-Kai Wan, Shang-Fu Yuan, Qing Tang, De-en Jiang, and Quan-Ming Wang**

Abstract: *A 23-gold-atom nanocluster was prepared by $NaBH_4$-mediated reduction of a solution of PhC≡CAu and $Ph_3PAuSbF_6$ in CH_2Cl_2. The cluster composition was determined to be $[Au_{23}(PhC{\equiv}C)_9(Ph_3P)_6]^{2+}$ and single-crystal X-ray diffraction revealed that the cluster has an unprecedented Au_{17} kernel protected by three PhC_2-Au-C_2(Ph)-Au-C_2Ph motifs and six Ph_3P groups. The Au_{17} core can be viewed as the fusion of two Au_{10} units sharing a Au_3 triangle. Electronic structure analysis from DFT calculations suggests that the stability of this unusual 12-electron cluster is a result of the splitting of the superatomic 1D orbitals under D_{3h} symmetry of the Au_{17} kernel. The discovery and determination of the structure of the Au_{23} cluster demonstrates the versatility of the alkynyl ligand in leading to the formation of new cluster compounds.*

Atomically precise, ligand-protected metal nanoclusters, in particular those of gold, are interesting not only because of their often molecule-like structures and properties but also because of their applications in catalysis, biosensing, luminescence, and molecular electronics.[1–5] Gold nanoclusters protected by thiolate or/and phosphine ligands have been extensively studied,[6–21] but alkynyl-protected gold nanoclusters are just beginning to attract attention. Tsukuda et al. synthesized a series of alkynyl-protected gold nanoclusters with Au_xL_y compositions (L is an alkynyl ligand) by the direct ligation of phenylacetylene to preformed small Au clusters (Au:PVP, PVP = polyvinylpyrrolidone).[22,23] However, the structures of these alkynyl-protected gold nanoclusters have not been determined.

As frequently demonstrated for thiolate-protected gold nanoclusters, total structural determination is crucial to understanding the interfacial bonding and the correlation between structure and properties. An alkynyl ligand contains a C≡C group that can function as both σ and π donors in coordinating metals, which provides more diverse structural motifs in comparison to a thiolate. This point has been clearly made in a recent computational study which showed PhC≡C-Au-C≡C-Ph and PhC≡C-Au-C≡C(Ph)-Au-C≡C-Ph motifs are preferred on the Au(111) surface and the Au_{20} nanocluster with the interfacial π bonding between gold and the C≡C bond.[24] To date, only two alkynyl-protected gold nanoclusters have been structurally determined. Konishi et al. prepared a cluster $[Au_8(dppp)_4(RC{\equiv}C)_2]^{2+}$ from dialkynylation of $[Au_8(dppp)_4]^{2+}$, where a RC≡C group is terminally bound as a σ donor to a gold atom (dppp = 1,3-bis(diphenylphosphanyl)propane).[25] More recently, we have shown that the direct reduction of gold alkynyl precursors with $NaBH_4$ led to the isolation of $[Au_{19}(PhC{\equiv}C)_9(Hdppa)_3](SbF_6)_2$ (Hdppa = *N*,*N*-bis-(diphenylphosphino)amine).[26] The Au_{19} cluster has a Au_{13} icosahedral core protected by three PhC_2-Au-C_2(Ph)-Au-C_2Ph motifs and three Hdppa groups. This is the first time that such motifs were observed experimentally, but are they common in alkynyl-protected gold nanoclusters? The Au_{19} cluster is an 8-electron system according to the superatom complex model and is therefore a magic cluster. However, the question remains as to whether synthesis and single-crystal X-ray determination can access other sizes, magic numbers, or structural building blocks.

Herein, we report the synthesis and total structure determination of a novel alkynyl-protected gold nanocluster, $[Au_{23}(Ph_3P)_6(PhC{\equiv}C)_9](SbF_6)_2$ (**1**), featuring a unprecedented Au_{17} core (or kernel), PhC_2-Au-C_2(Ph)-Au-C_2Ph motifs, and 12 free electrons. Both geometric and electronic structural analyses of this new cluster will be presented.

The cluster was prepared from the reduction of a CH_2Cl_2 suspension containing PhC≡CAu and $Ph_3PAuSbF_6$ (2:1) by $NaBH_4$. The sample was firstly characterized by ESI-TOF-MS (Figure 1). The peak at *m*/*z* 3506.57 corresponds to $[Au_{23}(PhC{\equiv}C)_9(Ph_3P)_6]^{2+}$. Its isotopic distribution pattern is in perfect agreement with the simulated one. X-ray photoelectron spectroscopy (XPS) yielded a binding energy of 84.4 eV for Au $4f_{7/2}$ (see the Supporting Information, Figure S1), indicating the gold atoms in **1** are presented largely as Au^0 centers.

The structure of **1** was determined by single-crystal X-ray diffraction.[27] The dicationic cluster $[Au_{23}(PhC{\equiv}C)_9(Ph_3P)_6]^{2+}$ consists of 23 gold atoms, 9 phenylethynyl ligands, and 6 triphenylphosphine ligands. The top view of **1** is shown in Figure 2a. The structure has C_3 symmetry with a Au_{17} kernel surrounded by three PhC_2-Au-C_2(Ph)-Au-C_2Ph motifs, colored green, yellow, and red. These motifs are called staple motifs, in analogy to the RS-Au-SR-Au-SR motifs found in $Au_n(SR)_m$ clusters. The three staple motifs are arranged in an up and down pattern alternately to surround the Au core around the center, forming a helical configuration (Figure 2b). As illustrated in Figure 2c, three Ph_3P ligands are located at the top of the kernel and the other three are at the bottom, each coordinated to a gold atom. The very similar

[*] X.-K. Wan, S.-F. Yuan, Prof. Dr. Q.-M. Wang
State Key Lab of Physical Chemistry of Solid Surfaces
Collaborative Innovation Center of Chemistry for Energy Materials (iChEM), Department of Chemistry
College of Chemistry and Chemical Engineering
Xiamen University, Xiamen, 361005 (P.R. China)
E-mail: qmwang@xmu.edu.cn
Dr. Q. Tang, Prof. Dr. D. Jiang
Department of Chemistry, University of California
Riverside, CA, 92521 (USA)
E-mail: de-en.jiang@ucr.edu

[**] This work was supported by the 973 program (2014CB845603), the Natural Science Foundation of China (21125102, 21390390, and 21473139) and the University of California, Riverside.

Supporting information for this article is available on the WWW under http://dx.doi.org/10.1002/anie.201500590.

 © 2015 Wiley-VCH Verlag GmbH & Co. KGaA, Weinheim

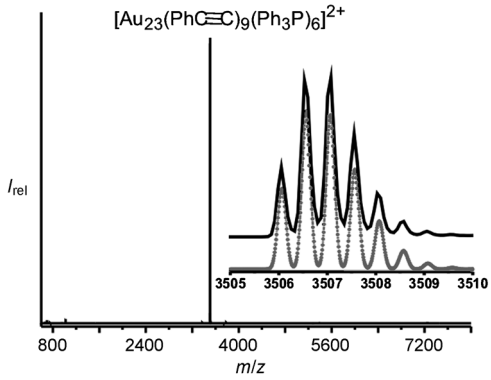

Figure 1. ESI-MS of **1**. Inset: the comparison of measured (solid trace, black) and simulated (dotted trace, gray) isotopic distribution patterns of $[Au_{23}(PhC{\equiv}C)_9(Ph_3P)_6]^{2+}$.

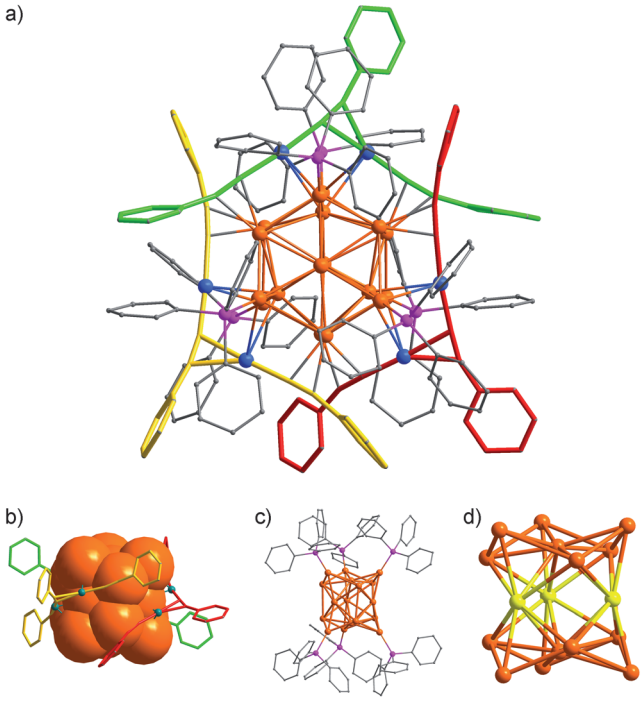

Figure 2. a) The crystal structure of $[Au_{23}(Ph_3P)_6(PhC{\equiv}C)_9]^{2+}$. Atom colors: orange = Au; blue = Au atoms of $Au_2(C_2Ph)_3$ motifs; purple = P; gray = C. Staple strands (PhC_2-Au-C_2(Ph)-Au-C_2Ph) are colored green, yellow, and red. b) Side view of the Au_{23} nanocluster with Ph_3P ligands removed. Au atoms are given as a space-filling model. c) The coordination of phosphine ligands. Staple motifs have been removed for clarity. d) The Au_{17} kernel with the three shared gold atoms highlighted in yellow.

environments of the phosphine ligands are confirmed by ^{31}P NMR spectroscopy, in which just one singlet at $\delta = 49.17$ ppm is detected (Figure S2). The Au_{17} kernel has roughly D_{3h} symmetry, which can be viewed as the fusion of two traditional Au_{10} units[28] by sharing a Au_3 triangle (yellow atoms in Figure 2d). This is the first reported observation of a Au_{17} core. Previously, it has been shown that two Au_{13} and Au_{11} can fuse to give Au_{25} and Au_{20},[18,21b] respectively.

The Au atoms of the PhC_2-Au-C_2(Ph)-Au-C_2Ph or staple motifs are connected to the Au_{17} core with Au–Au bond lengths in the range of 2.8819(17)–3.1022(18) Å. Within the Au_{17} kernel, the two central Au atoms (Figure 2a, center) are bound to the others with bond lengths 2.6881(16)–2.8971(17) Å, which are longer than those radial Au–Au distances of 2.666(1)–2.740(2) Å found in $[Au_{10}Cl_3(PCy_2Ph)_6]^+$.[28] The remaining Au–Au bond lengths fall within the range 2.7044(17)–3.1196(18) Å.

All the phenylethynyl ligands are involved in the formation of dimeric PhC_2-Au-C_2(Ph)-Au-C_2Ph staple motifs. The V-shaped motif was predicted by DFT on Au_{20} and is the same as those found in $[Au_{19}(PhC{\equiv}C)_9(Hdppa)_3](SbF_6)_2$.[24,26] The appearance of the dimeric PhC_2-Au-C_2(Ph)-Au-C_2Ph in $[Au_{23}(PhC{\equiv}C)_9(Ph_3P)_6]^{2+}$ indicates that the existence of such a motif could be ubiquitous in the alkynyl-protected gold nanoclusters of that size. It also suggests that staple motifs of other sizes, such as PhC_2-Au-C_2Ph (the monomer) and PhC_2-Au-C_2(Ph)-Au-C_2(Ph)-Au-C_2Ph (the trimer), could in the future prove to be the protecting motifs for new alkynyl-protected gold nanoclusters.

We found **1** to be very stable: it can be stored in the dark for more than a month without decomposition (Figure S3). To understand this stability, we analyzed the electronic structure of the cluster. The number of valence electrons of the $[Au_{23}(PhC{\equiv}C)_9(Ph_3P)_6]^{2+}$ cluster is $N^* = N_{Au} - N_{alkynyl} - Q = 23 - 9 - 2 = 12$, where Q is the cluster charge (+2), which is not a spherical shell-closing number. The stability of the cluster can be explained in terms of the unusual geometry of the cluster core. The 12 electrons of the cluster will fill the superatomic orbitals with the configuration of $(1S)^2(1P)^6(1D)^4$, so the key is to stabilize the four 1D electrons. The most efficient way is to split the fivefold degenerate 1D orbitals such that the HOMO orbitals are doubly degenerate and a sizable HOMO–LUMO gap can develop (HOMO = highest occupied molecular orbital, LUMO = lowest unoccupied molecular orbital). The D_{3h} symmetry of the Au_{17} core provides an orbital splitting as shown in Figure 3.[29] In this configuration, the energy level of the doubly degenerate HOMO orbitals ($D_{4,5}$) is notably lowered and populated by the four valence electrons. DFT calculations on the cluster confirmed this orbital picture (Figure 4). One can clearly see the d character of the five frontier orbitals. The whole cluster has C_3 symmetry; as a result, we found that a small splitting develops between the two orbitals of LUMO + 1 (about 0.09 eV).

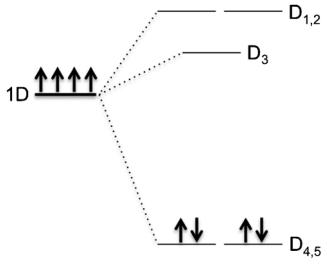

Figure 3. Splitting of the five 1D orbitals under D_{3h} symmetry and the population of the four valence electrons.

© 2015 Wiley-VCH Verlag GmbH & Co. KGaA, Weinheim

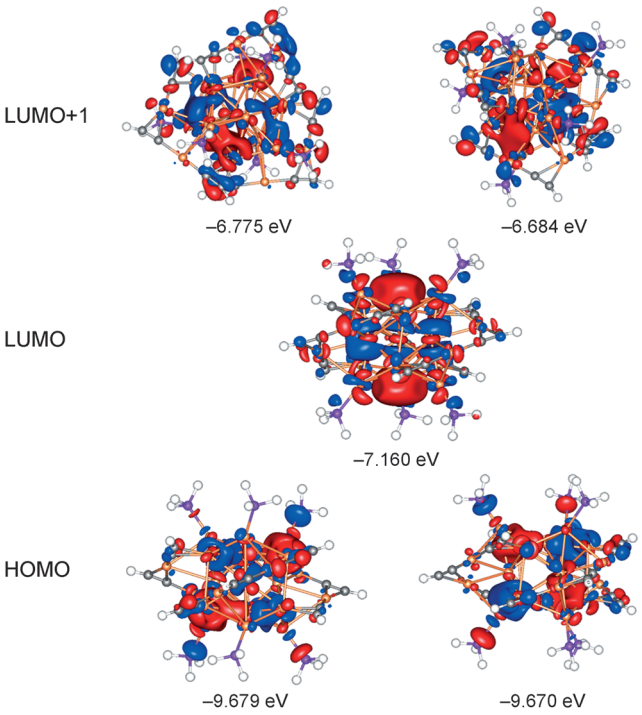

Figure 4. Frontier orbitals of $[Au_{23}(CH_3)_3P)_6(HC{\equiv}C)_9]^{2+}$. For computational efficiency, CH_3 was employed in place of Ph in the Ph_3P ligand and H- replaced Ph- in PhC≡C. Using the full Ph- ligands does not change the character and splitting of the frontier orbitals. Atom colors: orange = Au; purple = P; gray = C; white = H.

Figure 5 shows the comparison between the experimental and simulated (using time-dependent DFT) spectra. The three main features at 2.35, 2.75, and 3.20 eV from the experimentally determined spectrum are also evident in the simulated spectrum. The weak shoulder around 1.9 eV ($\varepsilon = 8356.9\,M^{-1}cm^{-1}$, where ε is the molar extinction coefficient) is attributed to the transition from HOMO to LUMO. For the 2.35 eV peak ($\varepsilon = 27696.7\,M^{-1}cm^{-1}$), the simulation yields a peak at 2.40 eV for this transition. Analysis of the orbitals involved shows that the transition is dominated by a contribution from HOMO (both orbitals) to LUMO + 1 (specifically the orbital at −6.684 eV, see Figure 4).

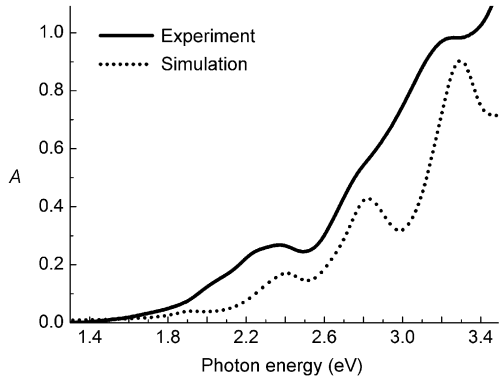

Figure 5. Experimental and simulated UV/Vis spectra. The simulated spectrum was calculated from time-dependent DFT at the B3LYP level. See the Supporting Information for computational details.

It is worth noting that previously there has been only one structurally determined ligand-protected gold nanocluster with 12 free electrons, $Au_{36}(SR)_{24}$, which has a tetrahedral Au_{28} core.[9] The five 1D orbitals in that structure split under the tetrahedral symmetry to a lower-energy doubly degenerate e_g orbital and a higher-energy triply degenerate t_{2g} orbital. The four 1D electrons occupy the two e_g orbitals, thereby lowering the energy of the cluster. In the case of the $[Au_{23}(PhC{\equiv}C)_9(Ph_3P)_6]^{2+}$ cluster reported herein, we have found an alternative way to stabilize the 12-electron system through the D_{3h} symmetry of the Au_{17} kernel.

It is also interesting to compare the $[Au_{23}(PhC{\equiv}C)_9(Ph_3P)_6]^{2+}$ cluster with a very different Au_{23} structure from $[Au_{23}(SR)_{16}]^-$ reported by Jin et al.,[14] where a bicapped cuboctahedral Au_{15} core is protected by two RS-Au-SR (monomer) and two RS-Au-RS-Au-SR-Au-SR (trimer) motifs together with four ordinary bridging SR ligands. The two Au_{23} clusters are different not only in geometric structures, but also in the number of valence electrons, a clear indication of ligand effects on the formation of individual nanoclusters.

In summary, this work demonstrates that alkynyl ligands can be particularly versatile in the protection of gold nanoclusters when combined with phosphine ligands. Our work further confirms the importance of the staple-dimer motif, PhC_2-Au-C_2(Ph)-Au-C_2Ph, at the surface of the cluster and calls for the discovery of staple motifs of different sizes. The electronic structure of the cluster demonstrates a new way to stabilize the 12 free electrons of the whole cluster and enables us to gain an understanding of the characteristics of the frontier orbitals and the optical transitions. We believe that by carefully tuning the structures of the alkynyl ligands and other protecting ligands, a variety of structures of gold and other coinage nanoclusters with various PhC_2-$[Au\text{-}C_2(Ph)]_x$ motifs ($x = 1$, or 3, or greater) can be discovered. We believe that this class of molecule-like metal nanoclusters has a bright future.

Experimental Section

Synthesis of **1**: To a solution of Ph_3PAuCl (24.7 mg, 0.05 mmol) in CH_2Cl_2 (2.0 mL), $AgSbF_6$ (17.2 mg, 0.05 mmol) in methanol (0.1 mL) was added with vigorous stirring. After 15 min stirring at room temperature, the resulting solution was centrifuged for 4 min at 10000 r min^{-1}, and the AgCl precipitate was filtered off. The solvent of the filtrate was removed under vacuum to give a colorless residue, which was dissolved in CH_2Cl_2 (4.0 mL). To this solution PhC≡CAu (29.8 mg, 0.1 mmol) was added, and then a freshly prepared solution of $NaBH_4$ (0.71 mg in 1.0 mL of ethanol) was added dropwise with vigorous stirring. The solution color changed from orange to pale brown and finally to dark brown. Then the reaction continued for 22 h at room temperature in air in the dark. The mixture was evaporated to dryness to give a black solid. The solid was washed with *n*-hexane (2 × 5 mL) and ether (2 × 5 mL), then dissolved in CH_2Cl_2 (2.2 mL), and the resulted solution was centrifuged for 4 min at 10000 r min^{-1}. The brown supernatant was collected and subjected to vapor diffusion with ether:*n*-hexane (v:v = 1:1) to afford black crystals after two weeks.

Keywords: alkyne ligands · cluster compounds · gold · nanoclusters · phosphines

 © 2015 Wiley-VCH Verlag GmbH & Co. KGaA, Weinheim

How to cite: *Angew. Chem. Int. Ed.* **2015**, *54*, 5977 – 5980
Angew. Chem. **2015**, *127*, 6075 – 6078

[1] G. Schmid, *Chem. Soc. Rev.* **2008**, *37*, 1909 – 1930.
[2] S. Yamazoe, K. Koyasu, T. Tsukuda, *Acc. Chem. Res.* **2014**, *47*, 816 – 824.
[3] G. Li, R. Jin, *Acc. Chem. Res.* **2013**, *46*, 1749 – 1758.
[4] M.-C. Daniel, D. Astruc, *Chem. Rev.* **2004**, *104*, 293 – 346.
[5] J. F. Parker, C. A. Fields-Zinna, R. W. Murray, *Acc. Chem. Res.* **2010**, *43*, 1289 – 1296.
[6] P. D. Jadzinsky, G. Calero, C. J. Ackerson, D. A. Bushnell, R. D. Kornberg, *Science* **2007**, *318*, 430 – 433.
[7] H. Qian, W. T. Eckenhoff, Y. Zhu, T. Pintauer, R. Jin, *J. Am. Chem. Soc.* **2010**, *132*, 8280 – 8281.
[8] D. Crasto, S. Malola, G. Brosofsky, A. Dass, H. Häkkinen, *J. Am. Chem. Soc.* **2014**, *136*, 5000 – 5005.
[9] C. Zeng, H. Qian, T. Li, G. Li, N. L. Rosi, B. Yoon, R. N. Barnett, R. L. Whetten, U. Landman, R. Jin, *Angew. Chem. Int. Ed.* **2012**, *51*, 13114 – 13118; *Angew. Chem.* **2012**, *124*, 13291 – 13295.
[10] C. Zeng, T. Li, A. Das, N. L. Rosi, R. Jin, *J. Am. Chem. Soc.* **2013**, *135*, 10011 – 10013.
[11] a) M. W. Heaven, A. Dass, P. S. White, K. M. Holt, R. W. Murray, *J. Am. Chem. Soc.* **2008**, *130*, 3754 – 3755; b) M. Zhu, C. M. Aikens, F. J. Hollander, G. C. Schatz, R. Jin, *J. Am. Chem. Soc.* **2008**, *130*, 5883 – 5885.
[12] A. Das, T. Li, K. Nobusada, Q. Zeng, N. L. Rosi, R. Jin, *J. Am. Chem. Soc.* **2012**, *134*, 20286 – 20289.
[13] Y. Song, S. Wang, J. Zhang, X. Kang, S. Chen, P. Li, H. Sheng, M. Zhu, *J. Am. Chem. Soc.* **2014**, *136*, 2963 – 2965.
[14] A. Das, T. Li, K. Nobusada, C. Zeng, N. L. Rosi, R. Jin, *J. Am. Chem. Soc.* **2013**, *135*, 18264 – 18267.
[15] C. Zeng, C. Liu, Y. Chen, N. L. Rosi, R. Jin, *J. Am. Chem. Soc.* **2014**, *136*, 11922 – 11925.
[16] B. K. Teo, X. Shi, H. Zhang, *J. Am. Chem. Soc.* **1992**, *114*, 2743 – 2745.
[17] J. Chen, Q.-F. Zhang, T. A. Bonaccorso, P. G. Williard, L.-S. Wang, *J. Am. Chem. Soc.* **2014**, *136*, 92 – 95.
[18] X.-K. Wan, Z.-W. Lin, Q.-M. Wang, *J. Am. Chem. Soc.* **2012**, *134*, 14750 – 14752.
[19] X.-K. Wan, S.-F. Yuan, Z.-W. Lin, Q.-M. Wang, *Angew. Chem. Int. Ed.* **2014**, *53*, 2923 – 2926; *Angew. Chem.* **2014**, *126*, 2967 – 2970.
[20] B. S. Gutrath, I. M. Oppel, O. Presly, I. Beljakov, V. Meded, W. Wenzel, U. Simon, *Angew. Chem. Int. Ed.* **2013**, *52*, 3529 – 3532; *Angew. Chem.* **2013**, *125*, 3614 – 3617.
[21] a) See Ref. [12]; b) Y. Shichibu, Y. Negishi, T. Watanabe, N. K. Chaki, H. Kawaguchi, T. Tsukuda, *J. Phys. Chem. C* **2007**, *111*, 7845 – 7847.
[22] a) P. Maity, H. Tsunoyama, M. Yamauchi, S. Xie, T. Tsukuda, *J. Am. Chem. Soc.* **2011**, *133*, 20123 – 20125; b) P. Maity, S. Takano, S. Yamazoe, T. Wakabayashi, T. Tsukuda, *J. Am. Chem. Soc.* **2013**, *135*, 9450 – 9457.
[23] P. Maity, T. Wakabayashi, N. Ichikuni, H. Tsunoyama, S. Xie, M. Yamauchi, T. Tsukuda, *Chem. Commun.* **2012**, *48*, 6085 – 6087.
[24] Q. Tang, D.-e. Jiang, *J. Phys. Chem. C* **2015**, DOI: 10.1021/jp508883v.
[25] N. Kobayashi, Y. Kamei, Y. Shichibu, K. Konishi, *J. Am. Chem. Soc.* **2013**, *135*, 16078 – 16081.
[26] X.-K. Wan, Q. Tang, S.-F. Yuan, D.-e. Jiang, Q.-M. Wang, *J. Am. Chem. Soc.* **2015**, *137*, 652 – 655.
[27] Crystal data for the structure **1**·CH_2Cl_2·Et_2O, $C_{180}H_{135}F_{12}P_6Sb_2Au_{23}$·$CH_2Cl_2$·$Et_2O$ $a = 24.8071(6)$, $b = 23.0911(5)$, $c = 31.3474(7)$ Å, $V = 17956.5(7)$ Å^3, orthorhombic, space group $Pna2_1$, $Z = 4$, $T = 100$ K, 60967 reflections measured, 30257 unique ($R_{int} = 0.0772$), final $R_1 = 0.0607$, $wR_2 = 0.1285$ for 21171 observed reflections [$I > 2\sigma(I)$]. CCDC-1044649 (**1**) contains the supplementary crystallographic data for this paper. These data can be obtained free of charge from The Cambridge Crystallographic Data Centre via www.ccdc.cam.ac.uk/data_request/cif.
[28] C. E. Briant, K. P. Hall, A. C. Wheeler, D. M. P. Mingos, *J. Chem. Soc. Chem. Commun.* **1984**, 248 – 250.
[29] L. Pan, B. Song, J. Sun, L. Zhang, W. Hofer, S. Du, H.-J. Gao, *J. Phys. Condens. Matter* **2013**, *25*, 505502 – 505507.

Received: January 21, 2015
Revised: March 7, 2015
Published online: March 25, 2015

 © 2015 Wiley-VCH Verlag GmbH & Co. KGaA, Weinheim